Active Disturbance Rejection Control of Linear Induction Motor

F. Alonge[a], M. Cirrincione[b] F. D'Ippolito[a], M. Pucci[c], A. Sferlazza[a]

[a]Dipartimento di Energia, ingegneria dell'Informazione e modelli Matematici (DEIM), University of Palermo, Palermo, Italy.
{francesco.alonge, filippo.dippolito, antonino.sferlazza}@unipa.it.
[b]School of Engineering, University of the South Pacific, Laucala Campus, Suva, Fiji Islands.
m.cirrincione@ieee.org
[c]I.S.S.I.A. C.N.R. section of Palermo (Institute on Intelligent Systems for Automation), via Dante 12, Palermo 90128, Italy.
pucci@pa.issia.cnr.it

***Abstract*—This paper proposes the theoretical framework and the experimental application of the active disturbance rejection control to linear induction motors. Such a non-linear control technique can be viewed as a particular kind of input-output linearization control technique, where the non-linear transformation of the state is not a priori given by a model, while it is estimated on-line. Such an approach permits to cope with modelling errors as well as any uncertainty in the knowledge of the model parameters. The effectiveness of the proposed active disturbance rejection control law has been verified experimentally on a suitably developed test set-up.**

***Index Terms*—Linear induction motor, state feedback control, extended state observer, rejection of disturbances.**

Table I
LIST OF SYMBOLS

u_{sx}, u_{sy}	inductor voltages in the induced part flux reference frame;
i_{sx}, i_{sy}	inductor currents in the induced part flux reference frame;
ψ_{rx}, ψ_{ry}	induced part fluxes in the induced part flux reference frame;
f_e (f_{eb})	electromagnetic (braking) thrust;
f_r	load force;
$L_s(L_r)$	inductor (induced part) inductance;
L_m	3-phase magnetizing inductance;
$R_s(R_r)$	inductor (induced part) resistance;
T_r	induced part time constant;
σ	total leakage factor;
ω_r	electrical angular speed of the induced part;
v	mechanical linear speed;
a	mechanical linear acceleration;
p	pole-pairs;
τ_p	pole-pitch;
τ_m	inductor length;
M	inductor mass.

I. INTRODUCTION

Linear Induction Motors (LIMs) have been largely studied for several years [1], [2]. Among the main reasons of their interest there is the capability to develop a direct linear motion without the need of any gear-box for the motion transformation (from rotating to linear). This advantage presents, as counterpart, the disadvantage of an increase of complexity of the machine model, presenting the so-called dynamic end effects, which are caused by the relative motion between the short inductor and the induced part track. As a result, starting from the assumption that the Rotating Induction Machine (RIM) presents a dynamic space-vector model which is non-linear [3], the dynamic model of the LIM presents further significant non-linearities, caused by the dynamic end effects. These non-linearities result in additional difficulties in the control of the electromechanical variables. Although the LIM presents a far more complicated non-linear model than the RIM, the approach adopted in literature for its control has been usually to simply extend the classic control techniques from RIMs to LIMs. In particular, as for high performance control techniques, the corresponding versions of the Field Oriented Control (FOC) [4], [5], [6] or the Direct Thrust Control (DTC) [7] have been developed. These control techniques have been partially adapted from the RIM counterpart [3], so as to take into consideration the end effects of the LIMs. Recently also sensorless control techniques have been applied to the LIM [8] which has been partially adapted from the RIM counterpart [9], [10].

The control system theory, however, offers an important corpus of non-linear control methodologies for dealing with a highly non-linear system. Among them, one of the most promising is the so-called input-output Feedback Linearization (FL). Actually, few applications of non-linear control methods and in particular of input-output feedback linearization to RIM control are provided by the scientific literature [11], [12], [13]. The current state of the art is described in [14]. A very limited number of papers in literature deal with the FL of LIMs. Papers like [15], and [16] apply the FL control technique to LIMs, but by adopting the RIM dynamic model for the definition of the control law, with consequent limitations due to an inadequate model. Only recently, the input-output feedback linearization control has been addressed in a systematic way, by suitably adopting a dynamic model of the LIM taking into consideration its dynamic end effects [17]. In particular, [18], [19] define the theoretical framework of the FL control for LIMs and present the experimental results. [20] presents an improvement of [18], [19], where the proposed FL control has been made adaptive with respect to the variations of the inductor resistance.

In general, it can be stated that non-linear controllers based

978-1-5090-0737-0/16/$31.00

on the FL are derived following two steps. In the first step, the model of the system is led to a standard model consisting of a chain of integrators expressed in new state space coordinates, where an auxiliary control input is adopted. As a result, the true control input is the superposition of a non-linear function of the state and the auxiliary input. In absence of uncertainties and endogenous disturbances, the above non-linear function can be assumed known and, consequently, it can be suitably compensated. In the second step, a linear control technique such as "pole assignment" imposes the desired dynamics to the closed-loop system. In the FL, however, the state-feedback computed analytically suffers from an evident problem arising from the uncertainties on both the dynamic model and its parameters, characterized by a significant complexity, see [18]. A way to overcome such a limitation of the FL, independently from the plant to be controlled, is the adoption of the so called Active Disturbance Rejection Control (ADRC) [21], [22], [23]. On this basis, this paper proposes the application of the ADRC to LIMs. To the best of the authors knowledge, such a control technique has never been applied to LIM control: actually only few examples of the ADRC are shown in literature applied to the RIM [24], [25].

In ADRC, the order of the dynamic model of the system is augmented, consisting of a chain of integrators in which the last equation expresses the dynamics of the above mentioned non-linear function of the state, permitting the model to be linearized. While in the classic FL method this function is assumed known, in the ADRC method this function is estimated by means of an Extended State Observer (ESO), permitting the non-linearity of the plant to be compensated. It follows that ADRC could be considered as an "adaptive robust version" of the FL control technique, since the state feedback term is estimated on-line. In this way, not only are the problems due to the uncertainties on the parameters addressed, but also possible problems of unmodelled dynamics are inherently sorted out.

The application of this control technique to the LIM is more significant than to the RIM, since the dynamic model of the LIM presents additional significant non-linearities caused by the dynamic end effects, leading to far more complex feedback terms. To this aim, an adaptive estimation will made the control algorithm more robust, because it is not necessary to take explicitly into consideration all the non-linearity effects and variations of the parameters during the different working conditions.

The paper is organized as follows. In section II the space-vector of the LIM including end effects is given. Section III deals with the ADRC law and it constitutes the main part of this paper. It is divided into three parts: in the first the extended models are defined, in the second the ESOs are designed for the previously defined extended models, and in the third two state feedback linear controllers are designed so that the induced part flux and the speed loops can satisfy the assigned requirements. Finally in Section IV the proposed ADRC has been tested and validated experimentally on a suitably developed test set-up.

II. Space-vector State Model of the LIM including end effects

The ADRC of LIMs is derived from the inductor and induced part voltage equations of the LIM including the end effects, as represented in [17]. If, among the different possibilities, a reference frame rotating at the speed of the induced part flux is chosen, with the direct axis x aligned with the induced part flux space-vector, the following equations can be written:

$$\frac{di_{sx}}{dt} = -\gamma i_{sx} + \frac{p\pi}{\tau_p} v i_{sy} + \frac{\alpha \hat{L}_m i_{sy}^2}{\psi_r} + \beta\alpha\psi_r + \frac{u_{sx}}{\hat{\sigma}\hat{L}_s}, \quad (1)$$

$$\frac{di_{sy}}{dt} = -\gamma i_{sy} - \frac{p\pi}{\tau_p} v i_{sx} - \frac{\alpha \hat{L}_m i_{sy} i_{sx}}{\psi_r} - \beta\frac{p\pi}{\tau_p} v\psi_r + \frac{u_{sy}}{\hat{\sigma}\hat{L}_s}, \quad (2)$$

$$\frac{d\psi_r}{dt} = -(\alpha - \eta)\psi_r + \alpha \hat{L}_m i_{sx}, \quad (3)$$

$$\frac{d\rho}{dt} = \frac{p\pi}{\tau_p} v + \frac{\alpha \hat{L}_m i_{sy}}{|\psi_r|}, \quad (4)$$

$$\frac{dv}{dt} = \mu(\psi_r i_{sy}) - \frac{F_r}{M} - \frac{F_{eb}}{M}, \quad (5)$$

$$F_{eb} = \vartheta\left[\psi_r^2 + L_{\sigma r}^2(i_{sx}^2 + i_{sy}^2) + L_{\sigma r}(\psi_r i_{sx})\right], \quad (6)$$

where $\psi_r = \psi_{rx}$ and $\psi_{ry} = 0$. The variables α, β, γ, η, μ and ϑ are defined as follow:

$$\alpha = \left(\frac{1}{\hat{T}_r} - \frac{\hat{R}_r}{\hat{L}_m}\right);\ \beta = \frac{\hat{L}_m}{\hat{\sigma}\hat{L}_s\hat{L}_r};\quad \eta = -\frac{\hat{R}_r}{\hat{L}_m};$$

$$\mu = \frac{3}{2} p \frac{\pi}{\tau_p}\frac{\hat{L}_m}{\hat{L}_r}\frac{1}{M};\quad \vartheta = \text{sign}(v)\frac{3}{2}\frac{L_r}{\hat{L}_r^2}\frac{1-e^{-Q}}{p\tau_p};$$

$$\gamma = \frac{1}{\hat{\sigma}\hat{L}_s}\left[R_s + \hat{R}_r\left(1 - \frac{\hat{L}_m}{\hat{L}_r}\right) + \frac{\hat{L}_m}{\hat{L}_r}\left(\frac{\hat{L}_m}{\hat{T}_r} - \hat{R}_r\right)\right].$$

For the definition of the symbols as well as of the speed dependent electrical parameters of the LIM, please see Table I.

It should be noted that, differently from RIM case, where all coefficients are constant, in the LIM case they are all speed dependent and thus time-varying parameters. As for the definition of the speed-varying electrical parameters (symbols with "ˆ"), the reader can refer to [17]. Moreover, F_{eb} is a term which does not exist in the RIM counter part, and it influences significantly the speed dynamic. This justifies the use of the ADRC technique in the LIM more then in the RIM when a linearization procedure is used in order to increase the dynamic performance. Indeed, in the FL control technique of LIM [18] very complex state feedback terms are considered, moreover the parameters of these terms are time varying due to the end-effects. However, in the ADRC approach the state feedback terms are estimated on-line by means of two ESOs, so all the non-linearity, uncertainties and variations of the parameters due to the end effects have not be taken into consideration directly, while they have been compensated adaptively.

III. The active disturbance rejection control law

The ADRC approach is based on the construction of an extended model of order $n+1$, where n is the order of the system to be controlled. An additional state variable representing the total disturbance consisting of parameter uncertainties, external disturbances and non-linearities must be properly defined. The model, in the end, is expressed in a canonical form consisting of a chain of integrators. Then an Extended State Observer (ESO) must be designed, so to be able to estimate the total disturbance. Finally, a control law is determined consisting of two components, the first compensates the total disturbance and the second assigns the desired behavior to the system.

A. Extended models

Two distinct extended models are proposed, i.e. the flux extended model and the speed extended model. The first consists of the equations of model (1)-(6) expressing the dynamics of the direct component of the inductor current and the induced part flux, and the other consists of the equations expressing the dynamics of the quadrature component of the inductor current and the speed.

1) Flux extended model: From model (1)-(6), using the linearization procedure used in [18], and defining $x_{\psi 1} = \psi_r$, and $x_{\psi 2} = \dot{\psi}_r$, the following equations can be written:

$$\dot{x}_{\psi 1} = x_{\psi 2}, \qquad \dot{x}_{\psi 2} = f + b_\psi u_{sx}. \tag{7}$$

where f is called *total flux disturbance* and it is defined as follows:

$$f = -q_1\psi_r + (\alpha-\eta)^2\psi_r - \alpha\hat{L}_m(\alpha-\eta)i_{sx} + q_2 i_{sx} - \alpha\hat{L}_m\gamma i_{sx} + \alpha\hat{L}_m\frac{p\pi}{\tau_p}v i_{sy} + \frac{\alpha^2\hat{L}_m^2 i_{sy}^2}{|\psi_r|} + \hat{L}_m\beta\alpha^2\psi_r, \tag{8}$$

with:

$$q_1 = \frac{R_r\hat{L}_r + R_r L_m(1+f(Q))}{\hat{L}_r^2}\cdot \cdot \frac{T_r a}{\tau_m}\left(1-\left(1+\frac{\tau_m}{T_r v}\right)e^{-\frac{\tau_m}{T_r v}}\right), \tag{9}$$

$$q_2 = R_r\left(\frac{L_m^2}{\hat{L}_r^2}(1+f^2(Q)) + 1 - 2\frac{L_m f(Q)}{\hat{L}_r}\right)\cdot \cdot \frac{T_r a}{\tau_m}\left(1-\left(1+\frac{\tau_m}{T_r v}\right)e^{-\frac{\tau_m}{T_r v}}\right), \tag{10}$$

while b_ψ is defined as: $b_\psi = \dfrac{\alpha\hat{L}_m}{\hat{\sigma}\hat{L}_s}$.

Now if an extra state variable $x_{\psi 3} = f$ is defined, the flux extended model becomes:

$$\dot{x}_{\psi 1} = x_{\psi 2}, \qquad \dot{x}_{\psi 2} = x_{\psi 3} + b_\psi u_{sx}, \qquad \dot{x}_{\psi 3} = \dot{f}. \tag{11}$$

2) Speed extended model: The procedure used for obtaining the speed extended model is analogous to that used for defining the flux extended model, while in this case the speed is assumed as measured output. Even in this case, from the model expressed by equations (1)-(6), using the linearization procedure used in [18], and defining $x_{v1} = v$ and $x_{v2} = \dot{v} = a$, the following equations can be written:

$$\dot{x}_{v1} = x_{v2}, \qquad \dot{x}_{v2} = \xi + b_v u_{sy}, \tag{12}$$

where ξ is called *total speed disturbance* defined as follows:

$$\xi = +\left(q_3 - \mu(\alpha-\eta)\right)\psi_r i_{sy} + \mu\alpha\hat{L}_m i_{sx} i_{sy} - \gamma\mu\psi_r i_{sy} + \left(q_4 - 2\frac{\vartheta}{M}(\alpha-\eta)\right)\psi_r^2 + \frac{\alpha\vartheta}{M}\hat{L}_m i_{sx} + L_{\sigma r}^2\left(q_2 - 2\frac{\gamma\vartheta}{M}\right)i_{sy}^2 - \left(\left(\mu\psi_r + 2\frac{\vartheta}{M}L_{\sigma r}^2\right)\left(\frac{p\pi}{\tau_p}v i_{sx} + \frac{\alpha\hat{L}_m i_{sy} i_{sx}}{|\psi_r|} + \beta\frac{p\pi}{\tau_p}v\psi_r\right)\right), \tag{13}$$

with:

$$q_3 = \frac{3}{2}p\frac{\pi}{\tau_p}\frac{1}{M}\left(-\frac{L_{\sigma r}L_m}{\hat{L}_r^2}\frac{T_r a}{\tau_m}\left(1-\left(1+\frac{\tau_m}{T_r v}\right)e^{-\frac{\tau_m}{T_r v}}\right)\right), \tag{14}$$

$$q_4 = \frac{3}{2}\frac{L_r}{\hat{L}_r^2}\frac{1}{p\tau_p M}\frac{a}{v}\left(\frac{L_m}{\hat{L}_r^2}\left(1-e^{-Q}\right)\left(f(Q)-e^{-Q}\right)\left(\hat{L}_r - L_m f(Q)\right) - Qe^{-Q}\right), \tag{15}$$

while b_v is defined as: $b_v = \dfrac{\mu\psi_r + 2\frac{\vartheta}{M}L_{\sigma r}^2}{\hat{\sigma}\hat{L}_s}$.

Now if an extra state variable $x_{\psi 3} = \xi$ is defined, the speed extended model becomes:

$$\dot{x}_{v1} = x_{v2}, \qquad \dot{x}_{v2} = x_{v3} + b_v u_{sy}, \qquad \dot{x}_{v3} = \dot{\xi}. \tag{16}$$

Models (11) and (16) show that the flux and speed extended models have the same structure. Moreover, choosing the control variables as follows:

$$u_{sx} = \frac{1}{b_\psi}\left(-\hat{x}_{\psi 3} + \nu_x'\right), \tag{17}$$

$$u_{sy} = \frac{1}{b_v}\left(-\hat{x}_{v3} + \nu_y'\right), \tag{18}$$

where $\hat{x}_{\psi 3}$ and $\hat{x}_{v3}$ are the estimates of $x_{\psi 3}$ and x_{v3}, respectively, and designing ν_x' and ν_y' so that the models (11) and (16) satisfy the design requirements, the total disturbances can be assumed as perfectly compensated. The estimates of the total disturbances are carried out by means of two ESOs. In particular two ESOs will be designed in order to estimate the state of the extended models and, as can be easily viewed from the model, the estimate of the total disturbance corresponds with the estimate of the third state variable.

Remark 1: On the basis of the above, the differences between the classic FL and the proposed ADRC technique

are clear. Indeed, in the classic FL the control inputs are also designed as in (17), but the total disturbances $f = x_{\psi 3}$ and $\xi = x_{v3}$ are analytically computed as in (8) and (13) with an evident problem arising from the uncertainties on the parameters due to the complexity of the formulation of (8) and (13). With the proposed ADRC, these terms are estimated as will be see in the following, and no-knowledge on the structure of these terms is needed. In this way not only the problems due to the uncertainties on the parameters are addressed, but also possible problems of unmodelled dynamics are sorted out.

Since the flux and speed extended models have the same structure, it is convenient to focus our attention on a general third-order extended model given by:

$$\dot{x}_1 = x_2, \qquad \dot{x}_2 = x_3 + bu, \qquad \dot{x}_3 = \dot{h}, \tag{19}$$

where h and x_1 are, respectively, the total disturbance and the output. Then the obtained results for the model (19) will be particularized for the two models under study (11) and (16).

B. ESO for a third-order extended model

The ESO chosen for the state estimation of model (19), is that proposed in [23], whose set of equations is given by:

$$\begin{aligned}
\dot{\hat{x}}_1 &= \hat{x}_2 - \epsilon g_1\left(\frac{\hat{x}_1 - x_1}{\epsilon^2}\right),\\
\dot{\hat{x}}_2 &= \hat{x}_3 - g_2\left(\frac{\hat{x}_1 - x_1}{\epsilon^2}\right) + bu,\\
\dot{\hat{x}}_3 &= -\epsilon^{-1} g_3\left(\frac{\hat{x}_1 - x_1}{\epsilon^2}\right),
\end{aligned} \tag{20}$$

where ϵ is a suitable positive parameter, and the functions $g_i(\cdot)$, $i = 1, 2, 3$, can be either linear or non-linear functions.

Defining the estimation errors:

$$\eta_i = \frac{e_i}{\epsilon^{3-i}},\ i = 1, 2, 3, \tag{21}$$

the dynamics of the variables η_i are described by the equations:

$$\begin{aligned}
\epsilon\dot{\eta}_1 &= \eta_2 - g_1(\eta_1),\\
\epsilon\dot{\eta}_2 &= \eta_3 - g_2(\eta_1),\\
\epsilon\dot{\eta}_3 &= -\epsilon\dot{h} - g_3(\eta_1).
\end{aligned} \tag{22}$$

The structure of $g_i(\eta_1)$, $i = 1, 2, 3$, characterizes the ESO. In this paper, we consider the Linear ESO (LESO). With this last choice, fixing $g_i(\eta_1) = \beta_i\eta_1$, $i = 1, 2, 3$, with β_i positive constants, equations (22) can be written as follow:

$$\epsilon\ddot{\boldsymbol{\eta}} = \boldsymbol{A}\boldsymbol{\eta} + \epsilon\boldsymbol{b}\dot{h} \tag{23}$$

where $\boldsymbol{\eta} = \begin{bmatrix}\eta_1 & \eta_2 & \eta_3\end{bmatrix}^T$, $\boldsymbol{A} = \begin{bmatrix}-\beta_1 & 1 & 0\\ -\beta_2 & 0 & 1\\ -\beta_3 & 0 & 0\end{bmatrix}$, and $\boldsymbol{b} = \begin{bmatrix}0 & 0 & -1\end{bmatrix}^T$.

A Theorem showing the stability of model (23) is shown in [22]. This aspect is particularly important since the stability of of model (23) implies the convergence of the estimation error (21). In the following, these results will be particularized in order to be used for the flux and the speed extended models.

1) LESO for the flux extended model: The flux extended model can be easily obtained putting $x_i = x_{\psi i}$, for $i = 1, 2, 3$, $h = f$ and $b = b_\psi$. The variable $x_1 = x_{\psi 1}$ is assumed known and, as it will be seen in the follows, it is given by a suitable observer. The parameters $\beta_i = \beta_{\psi i}$, for $i = 1, 2, 3$, are obtained so that the eigenvalues of the matrix $\boldsymbol{A}$ of model (23) belong to the left half part of the complex plane. In order to simplify the design, the three eigenvalues are chosen real and coincident. More precisely, the characteristic polynomial of $\boldsymbol{A}$, is given by:

$$\Delta_\psi(\lambda) = \lambda^3 + \beta_{\psi 1}\lambda^2 + \beta_{\psi 2}\lambda + \beta_{\psi 3} = (\lambda + \omega_\psi)^3, \tag{24}$$

where ω_ψ is the bandwidth to be assigned to the LESO for the flux model.

2) LESO for the speed extended model: The speed extended model can be easily obtained putting $x_i = x_{vi}$, for $i = 1, 2, 3$, $h = \xi$ and $b = b_v$. The variable $x_1 = x_{v1}$ is the measured speed, and the parameters $\beta_i = \beta_{vi}$, for $i = 1, 2, 3$, are chosen as said for the flux extended model. More precisely, the characteristic polynomial of $\boldsymbol{A}$, is given by:

$$\Delta_v(\lambda) = \lambda^3 + \beta_{v1}\lambda^2 + \beta_{v2}\lambda + \beta_{v3} = (\lambda + \omega_v)^3, \tag{25}$$

where ω_v is the bandwidth to be assigned to the LESO for the speed model.

C. Design of flux and speed controllers

As explained above, the flux and speed extended models have the same structure (19). It follows that also the flux and speed controllers will have the same structure and can be designed using the same approach. As in the ESO design, a controller for the system (19) is initially shown, and it specializes for the two previously defined controllers. With reference to (19), if $\hat{x}_3 \approx x_3$, the control law becomes:

$$u = \frac{1}{b}\left(-\hat{x}_3 + u_0\right), \tag{26}$$

leading to the model:

$$\dot{x}_1 = x_2, \qquad \dot{x}_2 = u_0. \tag{27}$$

Such a structure corresponds to a double integrator. This model is reachable and, consequently, a state feedback control law based on the assignment of the eigenvalues can be derived, but, as well known, it does not allow steady-state null errors to be obtained. Consequently, in order to have perfect tracking of constant reference the state of model (27) is augmented by adding a third variable z, whose dynamics is described as follows:

$$\dot{z} = x_{1ref} - x_1, \tag{28}$$

where x_{1ref} is the desired value of x_1. As it is easy to verify, model (27)-(28) is reachable and the control law:

$$u_0 = -\boldsymbol{k}^T\boldsymbol{x}, \tag{29}$$

with $\boldsymbol{k} = \begin{bmatrix}k_1 & k_2 & k_3\end{bmatrix}^T$ and $\boldsymbol{x} = \begin{bmatrix}x_1 & x_2 & z\end{bmatrix}^T$, allowing the eigenvalues of the dynamic matrix of the model to be

assigned. The characteristic polynomial of this matrix is given by:

$$\Delta(\lambda) = \lambda^3 + k_1\lambda^2 + k_2\lambda + k_3, \tag{30}$$

where the parameters k_1, k_2 and k_3 are determined assuming that the desired eigenvalues are $\lambda_1 = -\zeta\omega_n + j\omega_n\sqrt{1-\zeta^2}$, $\lambda_2 = -\zeta\omega_n - j\omega_n\sqrt{1-\zeta^2}$ and $\lambda_3 = \sigma$, where ω_n and ζ are the natural frequency and the damping factor respectively, while σ is a negative real number. Obviously, the implementation of the above control law can be carried out using the state estimated by the ESO. More precisely, the implementation of the control law requires the knowledge of x_1 and x_2, whereas the knowledge of x_3 allows to compensate the total disturbance h.

D. Design data of the ESO and controllers

The parameters of the ESOs and controllers are given below.

1) Flux model: : The ESO for flux is designed with $\omega_\psi = 5$ rad/s and $\epsilon = 0.05$. The parameters $\beta_i = \beta_{\psi i}$, for $i = 1, 2, 3$, are easily obtained from (24). The control law is given by (17) with $u_\psi = \boldsymbol{k}_\psi^T \boldsymbol{x}_\psi$, where $\boldsymbol{k}_\psi$ is determined so that the zeros λ_1, λ_2 and λ_3 of the polynomial (30) are chosen with $\omega_n = 10$, $\zeta = 0.9$ and $\sigma = -150$. The state is $\boldsymbol{x}_\psi = \begin{bmatrix} x_{\psi_1} & x_{\psi_2} & z_\psi \end{bmatrix}^T$ in which z_ψ is the output of an integrator supplied by the flux tracking error $\left(\psi_{rref} - x_{\psi_1}\right)$.

2) Speed model: : The ESO for speed is designed with $\omega_v = 5$ rad/s and $\epsilon = 0.05$. The parameters $\beta_i = \beta_{vi}$, for $i = 1, 2, 3$, are easily obtained from (25). The control law is given by (18) with $u_v = \boldsymbol{k}_v^T \boldsymbol{x}_v$, where $\boldsymbol{k}_v$ is determined so that the zeros λ_1, λ_2 and λ_3 of the polynomial (30) are chosen with $\omega_n = 12$, $\zeta = 1$ and $\sigma = -150$. The state is $\boldsymbol{x}_v = \begin{bmatrix} x_{v1} & x_{v2} & z_v \end{bmatrix}^T$ in which z_v is the output of an integrator supplied by the speed tracking error $(v_{ref} - x_{v1})$.

Obviously for the implementation of the presented control law, the induced part flux estimation is necessary. So, in order to cope with this problem, a suitable observer have to be designed. In this work the observer developed in [8] has been used, and it has been tuned by means of the procedure shown in [26].

IV. Test Set-up

A test set-up has been suitably built for the experimental verification of the proposed ADRC. The machine under test is a LIM model Baldor LMAC1607C23D99. The LIM has been equipped with a linear encoder Numerik Jena LIA series. The employed test set up consists of:

- A three-phase linear induction motor with parameters shown in Tab. II;
- A frequency converter which consists of a three-phase diode rectifier and a 7.5 kVA, three-phase VSI;
- A dSPACE card (DS1103) with a PowerPC 604e processor for fast floating-point calculation at 400 MHz and a fixed-point DSP TMS320F240.

The test set-up is equipped also with a torque controlled PMSM (Permanent Magnets Synchronous Motor) model Emerson Unimotor HD 067UDB305BACRA mechanically coupled to the LIM by a pulley-strap system, to determine an active load for the LIM. Fig. 1 shows a photograph of the test set-up.

Table II
Parameters of the LIM

Rated power P_{rated} $[W]$	425
Rated voltage U_{rated} $[V]$	380
Rated frequency f_{rated} $[Hz]$	60
Pole-pairs	3
Inductor resistance R_s $[\Omega]$	11
Inductor inductance L_s $[mH]$	637,6
Induced part resistance R_r $[\Omega]$	32,57
Induced part inductance L_r $[mH]$	757,8
3-phase magnetizing inductance L_m $[mH]$	517,5
Rated thrust F_n $[N]$	62
Rated speed $[m/s]$	6,85
Mass $[kg]$	20

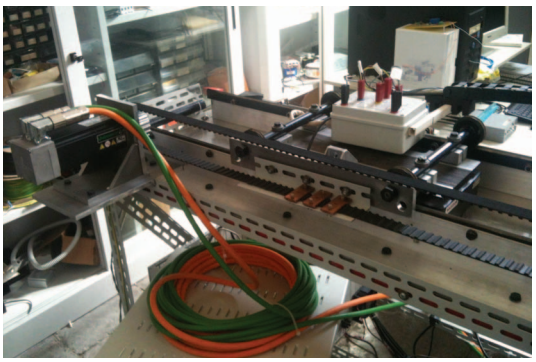

Figure 1. Photograph of the experimental test set-up.

V. Experimental Results

The proposed ADRC technique has been experimentally tested on the above described test set-up. As a first test, the LIM drive has been given a speed reference with a square waveform of magnitude equal to 0.3 m/s at no load. The frequency of such a square waveform is determined by the length of the induced part track. Whenever the inductor reaches the end of the track, the sign of the speed reference is inverted. Fig. 2,a shows the reference and measured linear speed of the LIM during such a test. Fig. 2,b shows the corresponding estimated induced part flux. Fig. 2,c shows the corresponding direct and quadrature components of the inductor currents, i_{sx}, i_{sy}. The correct behavior of the LIM drive can be observed with the measured speed suitably tracking its reference, with high dynamic performance. As for the induced part flux waveform, the ADRC correctly controls it at a constant value, with very small transient deviations with respect to the reference value of 0.8 Wb. As for the current waveforms, i_{sx} exhibits a waveform equal in shape and proportional in amplitude to that of the induced part flux, as expected, confirming the correct field orientation working condition. As for i_{sy}, it exhibits a waveform with step variations occurring in correspondence to each step variation of the reference speed, as expected, confirming the correct field orientation working condition.

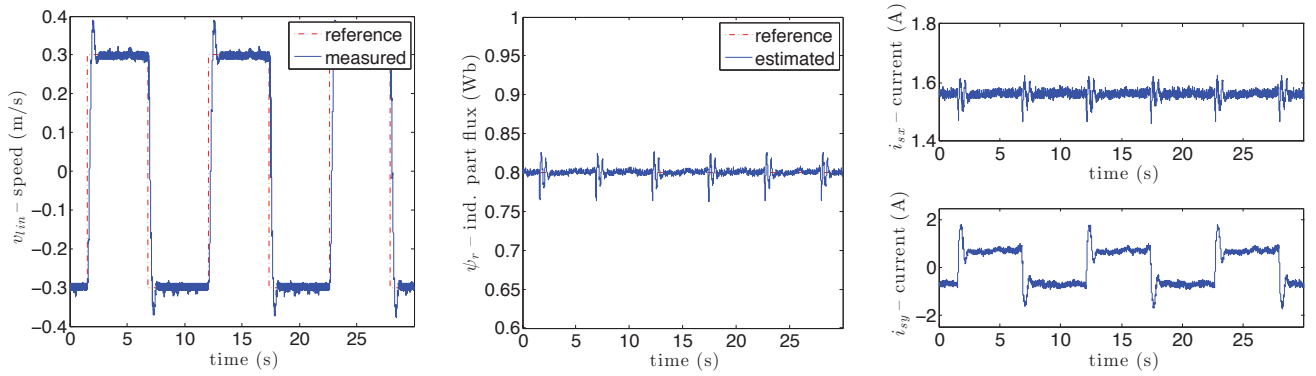

Figure 2. Linear speed of the drive (a), induced part flux amplitude (b) and currents i_{sx} and i_sy (c) during a speed reversal from 0.3 to $-0.3\,\mathrm{m\,s^{-1}}$.

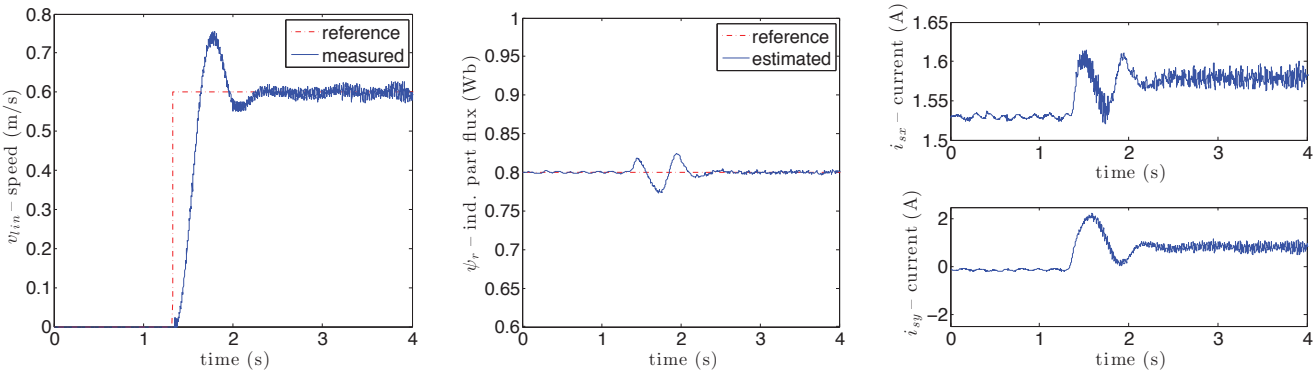

Figure 3. Linear speed of the drive (a), induced part flux amplitude (b) and currents i_{sx} and i_sy (c) during a start-up from 0 to $0.6\,\mathrm{m\,s^{-1}}$.

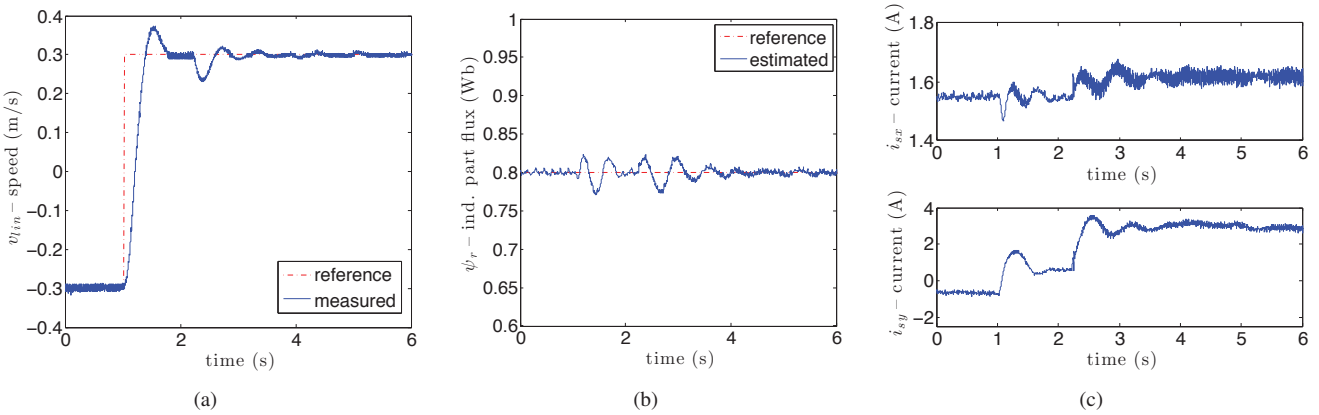

Figure 4. Linear speed of the drive (a), induced part flux amplitude (b) and currents i_{sx} and i_sy (c) during a test at $0.3\,\mathrm{m\,s^{-1}}$ with a load of 100 N.

Fig.s 3,a,b,c show the same kind of waveforms obtained during a start-up test of the drive from 0 to 0.6 m/s at no load. The analysis of all these waveforms shows the correct behavior of the drive under such working conditions and its high dynamic performance. Finally, Fig.s 4,a,b,c show the same kind of waveforms obtained during a a start-up test of the drive from 0 to 0.3 m/s after which a step load force of 100 N (close to the rated load of the LIM) is applied (after $t = 2$ s). It can be clearly observed that the speed controller immediately reacts to the application of the load force, with a null speed tracking error at steady-state (thanks to the above described structure of the linear controller). Correspondingly, the flux controller maintains the induced part flux constant, independently from the load. The i_{sy} current component exhibits a step increase subsequent to the application of the load force, as expected, to cope for the application of the load force, showing the correct

behavior of the speed control loop under the application of a load disturbance.

VI. Conclusion

This paper proposes the theoretical framework and the experimental application of the active disturbance rejection control to linear induction motors. Such a non-linear control technique can be viewed as a particular kind of input-output linearization control technique, where the non-linear transformation of the state is not a priori given by a model, while it is estimated on-line. Such an approach permits to cope with modelling errors as well as any uncertainty in the knowledge of the model parameters. The effectiveness of the proposed ADRC has been verified experimentally on a suitably developed test set-up.

References

[1] S. A. Nasar and I. Boldea, *Linear electric motors: theory, design, and practical application*. Prentice-Hall inc., 1987.

[2] I. Boldea and S. A. Nasar, "Linear electric actuators and generators," *Energy Conversion, IEEE Transactions on*, vol. 14, no. 3, pp. 712–717, 1999.

[3] W. Leonhard, *Control of electrical drives*. Springer, 2001.

[4] J.-h. Sung and K. Nam, "A new approach to vector control for a linear induction motor considering end effects," in *Industry Applications Conference, 1999. Thirty-Fourth IAS Annual Meeting. Conference Record of the 1999 IEEE*, vol. 4. IEEE, 1999, pp. 2284–2289.

[5] G. Kang and K. Nam, "Field-oriented control scheme for linear induction motor with the end effect," in *Electric Power Applications, IEE Proceedings-*, vol. 152, no. 6. IET, 2005, pp. 1565–1572.

[6] M. Pucci, "Direct field oriented control of linear induction motors," *Electric Power Systems Research*, vol. 89, pp. 11–22, 2012.

[7] I. Takahashi and Y. Ide, "Decoupling control of thrust and attractive force of a lim using a space vector control inverter," *Industry Applications, IEEE Transactions on*, vol. 29, no. 1, pp. 161–167, 1993.

[8] F. Alonge, M. Cirrincione, F. D'Ippolito, M. Pucci, A. Sferlazza, and G. Vitale, "Descriptor-type Kalman filter and TLS EXIN speed estimate for sensorless control of a linear induction motor," *IEEE Transactions on Industry Applications*, vol. 50, no. 6, pp. 3754–3766, 2014.

[9] F. Alonge and F. D'Ippolito, "Extended kalman filter for sensorless control of induction motors," in *2010 First Symposium on Sensorless Control for Electrical Drives*. IEEE, 2010, pp. 107–113.

[10] ——, "Robustness analysis of an extended kalman filter for sensorless control of induction motors," in *2010 IEEE International Symposium on Industrial Electronics*. IEEE, 2010, pp. 3257–3263.

[11] Z. Krzeminski *et al.*, "Nonlinear control of induction motor," in *10th IFAC World Congress*, vol. 349, no. 354. Munich, 1987, p. 33.

[12] D.-I. Kim, I.-J. HA, and M.-S. KO, "Control of induction motors via feedback linearization with input-output decoupling," *International Journal of Control*, vol. 51, no. 4, pp. 863–883, 1990.

[13] R. Marino, S. Peresada, and P. Valigi, "Adaptive input-output linearizing control of induction motors," *Automatic Control, IEEE Transactions on*, vol. 38, no. 2, pp. 208–221, 1993.

[14] R. Marino, P. Tomei, and C. M. Verrelli, *Induction motor control design*. Springer, 2010.

[15] F.-J. Lin and R.-J. Wai, "Robust control using neural network uncertainty observer for linear induction motor servo drive," *Power Electronics, IEEE Transactions on*, vol. 17, no. 2, pp. 241–254, 2002.

[16] R.-J. Wai and C.-C. Chu, "Robust petri fuzzy-neural-network control for linear induction motor drive," *Industrial Electronics, IEEE Transactions on*, vol. 54, no. 1, pp. 177–189, 2007.

[17] M. Pucci, "State space-vector model of linear induction motors," *Industry Applications, IEEE Transactions on*, vol. 50, no. 1, pp. 195–207, 2014.

[18] F. Alonge, M. Cirrincione, M. Pucci, and A. Sferlazza, "Input–output feedback linearizing control of linear induction motor taking into consideration the end-effects. Part I: Theoretical analysis," *Control Engineering Practice*, vol. 36, pp. 133–141, 2015.

[19] ——, "Input–output feedback linearizing control of linear induction motor taking into consideration the end-effects. Part II: Simulation and experimental results," *Control Engineering Practice*, vol. 36, pp. 142–150, 2015.

[20] ——, "Input–output feedback linearization control with on-line MRAS-based inductor resistance estimation of linear induction motors including the dynamic end effects," *IEEE Transactions on Industry Applications*, vol. 52, no. 1, pp. 254–266, 2016.

[21] J. Han, "From PID to active disturbance rejection control," *Industrial Electronics, IEEE transactions on*, vol. 56, no. 3, pp. 900–906, 2009.

[22] Y. Huang and W. Xue, "Active disturbance rejection control: methodology and theoretical analysis," *ISA transactions*, vol. 53, no. 4, pp. 963–976, 2014.

[23] B.-Z. Guo and Z.-l. Zhao, "On the convergence of an extended state observer for nonlinear systems with uncertainty," *Systems & Control Letters*, vol. 60, no. 6, pp. 420–430, 2011.

[24] J. Li, H.-P. Ren, and Y.-R. Zhong, "Robust speed control of induction motor drives using first-order auto-disturbance rejection controllers," *Industry Applications, IEEE Transactions on*, vol. 51, no. 1, pp. 712–720, 2015.

[25] L. Liu, Z. Xu, and Q. Mei, "Induction motor drive system based on ADRC and PI regulator," in *Intelligent Systems and Applications, 2009. ISA 2009. International Workshop on*. IEEE, 2009, pp. 1–4.

[26] F. Alonge, M. Cirrincione, F. D'Ippolito, M. Pucci, and A. Sferlazza, "Parameter identification of linear induction motor model in extended range of operation by means of input-output data," *Industry Applications, IEEE Transactions on*, vol. 50, no. 2, pp. 959–972, 2014.